Magnetic properties and spin dynamics in the Cr_7Fe nanomagnet: A heterometallic antiferromagnetic molecular ring

H. Amiri,[1,2,*] M. Mariani,[2] A. Lascialfari,[1,2,3] F. Borsa,[2] G. A. Timco,[4] F. Tuna,[4] and R. E. P. Winpenny[4,5]
[1]*Department of Molecular Sciences Applied to Biosystems, DISMAB, Università degli Studi di Milano, I-20134 Milan, Italy*
[2]*Department of Physics "A. Volta" and CNISM-INFM unit, Università di Pavia, I-27100 Pavia, Italy*
[3]*Centro S3, CNR-Istituto di Nanoscienze, I-41125 Modena, Italy*
[4]*The Lewis Magnetism Laboratory, School of Chemistry, The University of Manchester, Oxford Road, Manchester M13 9PL, United Kingdom*
[5]*The Photon Science Institute, The University of Manchester, Oxford Road, Manchester M13 9PL, United Kingdom*
(Received 14 December 2009; revised manuscript received 18 February 2010; published 15 March 2010)

We present magnetic susceptibility, ^{1}H nuclear magnetic resonance (NMR) spectra, spin-spin- and spin-lattice-relaxation rates data, collected in the temperature range $1.65 < T < 300$ K at two applied magnetic fields $H=0.35$ and 1.5 T, on a single crystal of Cr_7Fe heterometallic molecular nanomagnet. From a simple analysis of the magnetic susceptibility data, we deduce that the ring has a magnetic total spin $S_T=1/2$ ground state and Cr-Cr antiferromagnetic (AFM) exchange interactions comparable to similar Cr_7M heterometallic rings. The proton NMR data indicate that the main coupling between nuclei and electronic moments is of dipolar origin. The spin-lattice-relaxation rate behavior is qualitatively explained by a model which assumes a single-correlation time as used previously for homometallic AFM rings. The direct comparison of the relaxation data in Cr_7Fe and Cr_8 shows a substantial change in the spin dynamics as the result of Fe replacing one Cr ion. The difference is attributed to the change in the elastic properties of the sample with Fe substitution and/or to the multi-Lorentzian behavior of the spin-spin correlation function resulting from the presence of inequivalent ions in the heterometallic ring.

DOI: 10.1103/PhysRevB.81.104408 PACS number(s): 76.60.Es, 75.50.Xx

I. INTRODUCTION

The discovery of transition-metal complexes (magnetic molecules) which act as individual nanomagnets has opened a new field of research in the physics community.[1–3] In a nanomagnet the magnetic core of the individual molecules is shielded from each other by a shell of bulky organic ligands so that the intermolecular magnetic interactions (usually dipolar) are very weak compared to the intramolecular exchange interactions.[3] Therefore, measurements in these crystalline samples reflect the magnetic properties of one isolated molecule. As a result, these zero-dimensional nanomagnetic systems have become a unique platform for studying spin dynamical effects.

Antiferromagnetic (AFM) rings are magnetic molecules comprising an even number (N) of uniformly spaced paramagnetic metal ions arranged as a planar ring. If the ring contains just one type of magnetic ion then it is called homometallic (homonuclear), e.g., Cr_8, which is characterized by a singlet zero-field ground state with total spin $S_T=0$.[4] Recently it has been recognized that the substitution in the ring of one paramagnetic ion with a nonmagnetic ion or with an ion with different magnetic moment can generate heterometallic AFM rings, which reveal new interesting physics both in the static and in the dynamical magnetic properties.[5] One obvious consequence is the change in the ground state from a singlet with $S_T=0$ to a magnetic state with $S_T \neq 0$. Furthermore, the local spin moment in the ground state becomes redistributed in a staggered and nonuniform way.[6] Finally the ground state of these heterometallic AFM rings could be used for implementation of qubits for quantum computation and the synthesis of heterometallic rings containing coupled molecules could lead to quantum entanglement.[7,8] The investigation of the magnetic properties and particularly of the spin dynamics which can affect the quantum coherence or decoherence in these heterometallic rings is thus of paramount importance.

Nuclear magnetic resonance (NMR) has been proved to be an efficient local probe of both static and dynamic properties of magnetic molecules[9] and used in combination with thermodynamic magnetization measurements can give a good characterization of the magnetic properties and the spin dynamics in the heterometallic rings. In this paper we investigate the heterometallic molecular magnetic ring of formula $(C_4H_9)_2NH_2Cr_7Fe^{2+}F_8(O_2CCMe_3)_{16}$, in brief Cr_7Fe. In the ground state, this ring is characterized by a total spin $S_T=1/2$ resulting from AFM interactions J and J' between two Cr^{3+}, $s=3/2$, ions and between Cr^{3+} and Fe^{2+}, $s=2$, ions, respectively.

The paper is organized as follows. In Sec. II we summarize briefly the synthesis of the compounds and their crystal structure. In Sec. III we present the experimental results and data analysis for the magnetization. In Sec. IV we present in separate sections the static and the dynamic NMR results with their analysis. Section V contains a comparison between the heterometallic ring Cr_7Fe and the homometallic ring Cr_8 and a discussion of the results obtained with the different techniques and the relevant conclusions. We will show that the spin dynamics in the heterometallic ring Cr_7Fe differs substantially from the one of homometallic Cr_8.

II. SYNTHESIS AND STRUCTURE

The homometallic ring, $[Cr_8F_8(O_2CCMe_3)_{16}]$, has been widely studied,[10] both because of its magnetic properties[11]

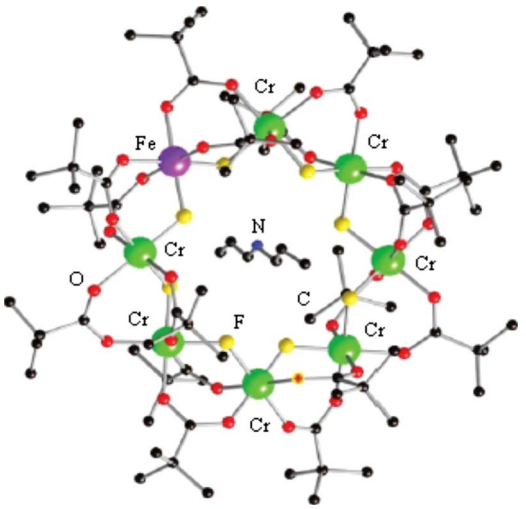

FIG. 1. (Color online) Structure of $(C_4H_9)_2NH_2$ $Cr_7Fe^{2+}F_8(O_2CCMe_3)_{16}$ nanomagnet, in brief Cr_7Fe.

and because it can act as a host for heterometallic substitution.[12] In order to prepare a heterometallic ring one of the chromium ions should be substituted with a metallic ion.[5] For this, $CrFe_3 \cdot 4H_2O$ (5.0 g, 27.6 mmol), di-n-butylamine (1.43 g, 11.1 mmol), and pivalic acid (14.0 g, 137.1 mmol) were heated to 140 °C while stirring for 1.5 h in an open teflon flask. Then the following procedures were performed under nitrogen atmosphere. The $FeCl_2 \cdot 4H_2O$ (1.5 g, 7.5 mmol) was added to the mixture and the temperature was increased to 160 °C for 5 h, at which point a green crystalline product had formed. The flask was cooled to room temperature and acetone (50 mL) was added while stirring. The product was collected by filtration, washed with a large quantity of acetone, then dried *in vacuo* and then purified by column chromatography on silica gel using as the eluent toluene. The compound $(C_4H_9)_2NH_2Cr_7Fe^{2+}F_8(O_2CCMe_3)_{16}$ elutes as the second fraction then crystallized by evaporation of the toluene. Yield: 6.04 g (66%, based on Cr). Elemental analysis calculated (%) for $C_{88}H_{164}Cr_7F_8FeNO_{32}$: Cr 15.69, Fe 2.41, C 45.56, H 7.12, N 0.60, and F 6.55; found: Cr 15.35, Fe 2.37, C 46.88, H 7.10, N 0.52, and F 6.51. Electrospray-MS (THF/MeOH) m/z: $-2188[Cr_7FeF_8(O_2CCMe_3)_{16}]^-$; $+2320[M^+]$; $+2342[M+Na]^+$.

The schematic structure of Cr_7Fe ring is shown in Fig. 1. The position of protons in the molecule is important for our ^1H NMR study. Around each Cr there are three closest CH_3 groups. For each CH_3 there are three Cr-H distances: (i) shortest, fall in the range of 4.07–4.32 Å, (ii) middle, fall in the range of 4.48–4.93 Å, and (iii) longest, fall in the range of 5.47–5.57 Å. Other protons are located even further away from Cr ions.

III. MAGNETIC SUSCEPTIBILITY

Measurements of magnetic susceptibility, i.e., $\chi \approx (M/H)_{H\to 0}$ ($\equiv M/H$ for paramagnets, like our case) have been performed with a superconducting quantum interference device (SQUID) magnetometer on Cr_7Fe single crystals, at two different external magnetic fields $H=0.35$ and 1.5 T, applied parallel and perpendicular to the molecular c axis. The c axis is perpendicular to the plane formed by the magnetic ions, i.e., to the plane of the ring. The results, corrected for the small single-ion diamagnetism (5.8×10^{-4} emu/mol), are shown in Fig. 2. The results should be analyzed in terms of a Heisenberg Hamiltonian including the AFM coupling J between the seven nearest-neighbor Cr^{3+} ($s=3/2$) ions and a different coupling J' between the two pairs of Cr^{3+}-Fe^{2+} ions where Fe^{2+} carries a spin $s=2$. Small single-ion anisotropy may be also present as revealed by the susceptibility data collected at two orientations of the external field (see Fig. 2).

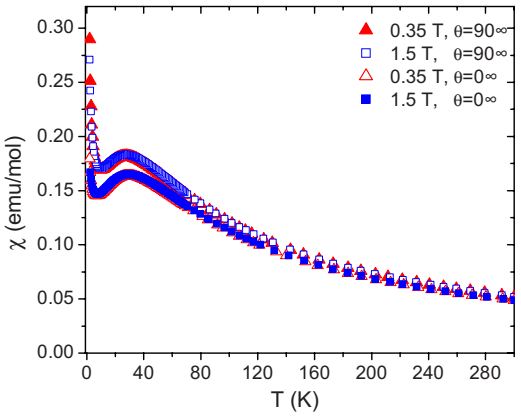

FIG. 2. (Color online) Magnetic susceptibility vs temperature in a single-crystal sample of Cr_7Fe at the same external magnetic fields used in NMR, both parallel (angle between H and c axis: $\theta=0°$) and perpendicular ($\theta=90°$) to the molecular axis.

For a detailed and complete characterization of the magnetic structure and properties, neutron-scattering data would be necessary as in the case of Cr_7Ni (Ref. 13). A preliminary simplified analysis is, however, sufficient for the purpose of the present work which is mostly focused on the spin dynamics obtained by NMR measurements. For this purpose we show in Fig. 3 a plot of the effective Curie constant $C=\chi T$ as a function of temperature.

Both in Figs. 2 and 3 there appear to be a small difference in the susceptibility between the parallel and the perpendicular orientations of the external magnetic field. We will neglect this anisotropy in the analysis which follows. The upper dashed line ($C=16.32$) in Fig. 3 corresponds to the value of the Curie constant $C=Ng^2\mu_B^2[s(s+1)]/3k_B$ where it was assumed for the gyromagnetic ratio $g=2$ for both Cr^{3+} and Fe^{2+} ions while the spin s is 3/2 and 2, respectively. The experimental data in Fig. 3 lie below the high-T limit as expected in presence of AFM coupling but seem to bend towards the limit calculated for noninteracting ions with the given spin s value and negligible single-ion anisotropy ($g=2$). The low-temperature dashed line represents the Curie constant for a single spin, $S_T=1/2$, with $g=2$. Again the agreement is good indicating that the ground state is a magnetic state, $S_T=1/2$, with small anisotropy.

In Fig. 4 we plot the inverse susceptibility vs temperature in order to derive an estimate of the AFM coupling constants J and J' between nearest-neighbor magnetic ions in the ring.

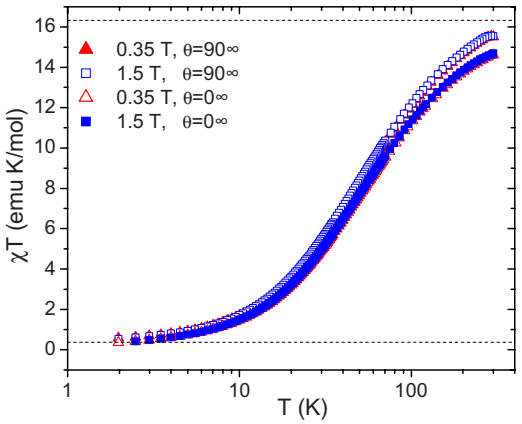

FIG. 3. (Color online) The product of the susceptibility times temperature plotted vs temperature in Cr_7Fe at two external magnetic fields both parallel ($\theta=0°$) and perpendicular ($\theta=90°$) to the molecular axis. The dashed lines are the limiting behaviors at high and low temperatures, respectively, expected for a simple AFM ring model (see text).

The high-temperature results can be fitted reasonably well by using a Curie-Weiss law for the susceptibility, i.e., $1/\chi=[T+\Theta]/C$, with $C=16.32$ as calculated above for the high-T limit in Fig. 3 and choosing the only fitting parameter to be $\Theta=-32\pm2$ K.

Assuming that the dominant contribution to the Curie-Weiss temperature Θ comes from the more abundant Cr^{3+} ions and using the molecular field approximation expression $\Theta=[2zs(s+1)J]/3k_B$, with the number of nearest neighbors of a given moment being $z=2$, one gets an AFM coupling constant $J/k_B=-6.4\pm0.4$ K.

The exchange constant J derived above corresponds to a Hamiltonian for the Heisenberg model written as $\Sigma_{i>j}-2J_{ij}\vec{S}_i\cdot\vec{S}_j$. Since the values of J given in molecular nanomagnets are normally referred to a Hamiltonian written as $\Sigma_{i>j}J_{ij}\vec{S}_i\cdot\vec{S}_j$, we multiply our value by two and change sign in order to compare it with the J constants given in the literatures for AFM rings. For other heterometallic rings such as Cr_7Zn, Cr_7Ni, and Cr_7Mn as well as for the homometallic ring Cr_8 (Refs. 13 and 14) the exchange constant between adjacent Cr ions is found to be approximately the same, namely, $J_{Cr\text{-}Cr}=17\pm0.5$ K. The value estimated above from the high-temperature Curie-Weiss law for Cr_7Fe is smaller, i.e., $J=13\pm1$ K, but this can be due to the neglecting of Cr-Fe exchange coupling, which could be smaller than the Cr-Cr one, and to the approximate model we have used for the susceptibility.

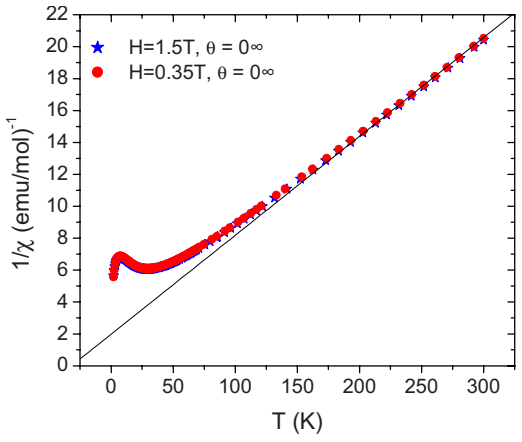

FIG. 4. (Color online) Inverse susceptibility vs T in Cr_7Fe with the external magnetic fields parallel ($\theta=0°$) to the molecular axis; the solid line is a fit according to the Curie-Weiss law (see text).

IV. NMR EXPERIMENTAL RESULTS AND ANALYSIS

Proton NMR measurements on Cr_7Fe powder sample (single crystals are too small to give detectable signals) including nuclear spin-lattice-relaxation time (T_1) and spin-spin-relaxation time (T_2) were performed using a standard TecMag Fourier transform pulse NMR spectrometer with short $\pi/2$-$\pi/2$ radio frequency pulses (1.9–2.2 μs) in the temperature range $1.65<T<300$ K at two applied magnetic fields: $H=0.35$ and 1.5 T. In order to study the temperature dependence of the relaxation times, we used two different cryostats: (a) a continuous flow cryostat in the temperature range $4.2<T<300$ K and (b) a bath cryostat in the temperature range $1.65<T<4.2$ K. Fourier transform of half of the echo spin signal yields the NMR spectrum in the case where the whole line could be irradiated with one radio frequency (rf) pulse.

The nuclear spin-lattice-relaxation rate T_1^{-1} was determined by monitoring the recovery of the longitudinal nuclear magnetization measured by the spin echo amplitude obtained with $\pi/2$-$\pi/2$ Hahn echo reading sequence, following a saturating comb of rf pulses. The length of the rf saturation comb was chosen to ensure the best initial saturation conditions, which vary depending on temperature and resonance frequency.

To perform the spin-spin-relaxation time experiments, a standard solid echo ($\pi/2$-$\pi/2$) pulse sequence was used. For all temperatures a monoexponential behavior was observed so that a well-defined spin-spin-relaxation time parameter T_2 was extracted from the decay of the transverse proton magnetization.

On the other hand the recovery after saturation of the longitudinal component of the nuclear magnetization was found to follow a nonexponential law. Thus we obtained T_1 values using the slope of the tangent at the origin of the semilogarithmic recovery plot of the nuclear magnetization. This corresponds to measure the average value of the relaxation rate T_1^{-1} over all the nuclei irradiated.[9] The recovery of the nuclear magnetization below 3.8 K displays an initial fast recovery followed by a very slow recovering tail. In view of the difficulty in interpreting the recovery curve we decided not to include in the presentation the very low-temperature data.

A. Proton NMR spectra

The proton NMR linewidth full width at half maximum (FWHM) or $\Delta\nu$ is shown in Fig. 5(a) as a function of temperature at two values of the external magnetic field. The shape and width of the proton NMR spectrum are determined

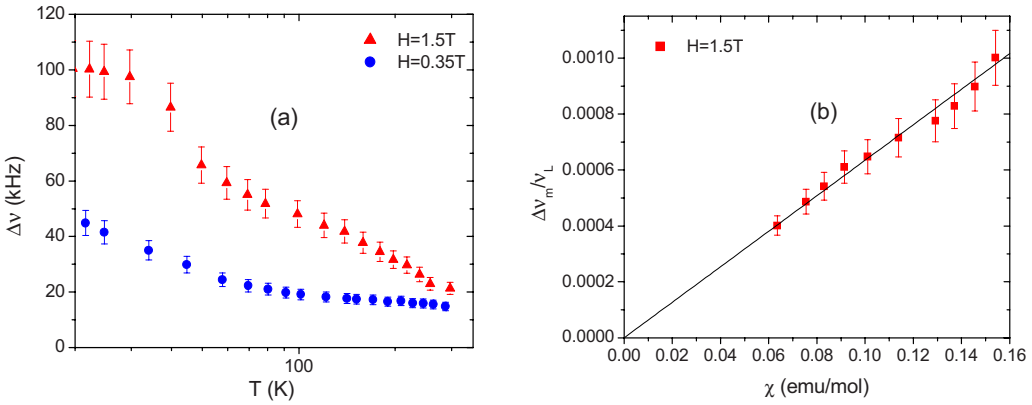

FIG. 5. (Color online) (a) Proton linewidth vs temperature in Cr_7Fe at two different external magnetic fields; (b) inhomogeneous part of the linewidth, extracted as explained in the text, plotted vs magnetic susceptibility with temperature as implicit parameter.

by two main interactions: (i) the nuclear-nuclear dipolar interaction and (ii) the hyperfine interaction of the proton with the neighboring magnetic ions. The first interaction generates a temperature- and field-independent broadening, which depends on the hydrogen distribution in the molecule and is thus similar in all molecular magnets independently of their magnetic properties.[9]

The hyperfine field resulting from the interaction of protons with local magnetic moments of Cr^{3+} (Fe^{2+}) may contain contributions from both the classical dipolar interaction and from a direct contact term due to the hybridization of proton *s*-wave function with the *d*-wave function of magnetic ions. The dipolar contribution has tensorial character and is thus responsible for the inhomogeneous width of the line due to the random distribution of orientations in a powder sample and to the many nonequivalent proton sites in the single crystal. The contact interaction, on the other hand, has scalar form and it can generate a shift of the line for certain groups, each one constituted by equivalent protons in the molecule. Since we have not observed any measurable shift of the proton NMR line from the Larmor frequency, we can conclude that the dominant hyperfine interaction is of dipolar origin.

In the usual simple Gaussian approximation for the NMR line shape, the linewidth is proportional to the square root of the second moment, which in turn is given by the sum of the second moments due to the two interactions described above[15]

$$\mathrm{FWHM} \propto \sqrt{\langle \Delta \nu^2 \rangle_d + \langle \Delta \nu^2 \rangle_m}, \tag{1}$$

where $\langle \Delta \nu^2 \rangle_d$ is the intrinsic second moment due to nuclear-nuclear dipolar interactions, and $\langle \Delta \nu^2 \rangle_m$ is the second moment of the local frequency-shift distribution (due to nearby electronic moments) at the different proton sites of all molecules. The proportionality constant in Eq. (1) is of the order of one depending on the exact shape of the spectrum. We will assume it to be one for simplicity. The relation between $\langle \Delta \nu^2 \rangle_m$ and the local Cr^{3+}, Fe^{2+} electronic moments for a simple dipolar interaction is given by[9,15]

$$\langle \Delta \nu^2 \rangle_m = \frac{1}{N} \sum_R \left(\sum_{i \in R} \langle \nu_{R,i} - \nu_0 \rangle_{\Delta t} \right)^2 = \frac{\gamma^2}{N} \sum_R \left[\sum_{i \in R} \sum_{j \in R} \frac{A(\vartheta_{i,j})}{r_{i,j}^3} \langle m_{z,j} \rangle_{\Delta t} \right]^2, \tag{2}$$

where R labels different molecules, i and j span different protons and Cr^{3+} ions within each molecule, and N is the total number of probed protons. In Eq. (2), $\nu_{R,i}$ is the NMR resonance frequency of nucleus i and $\nu_L = (\gamma/2\pi)H = \gamma H$ is the bare Larmor resonance frequency. The difference between the two resonance frequencies represents the shift for nucleus i due to the local field generated by the nearby moments j. The angular-dependent dipolar coupling constant between nucleus i and electronic moment j is $A(\vartheta_{i,j})$ and $r_{i,j}$ is the corresponding distance. $\langle m_{z,j} \rangle$ is the component of the Cr (Fe) moment j in the direction of the applied field, averaged over the NMR data acquisition time. In a simple paramagnet one expects $\langle m_{z,j} \rangle = \frac{\chi}{N_A} H$ with χ the SQUID susceptibility in emu/mole, N_A Avogadro's number, and H the applied field.[16]

We can thus write approximately

$$\sqrt{\langle \Delta \nu^2 \rangle_m} = A_z' \chi H = A_z' \chi \nu / \gamma = A_z \chi \nu / N_A, \tag{3}$$

where A_z' and A_z are the dipolar coupling constants averaged over all protons and all orientations expressed in different units and ν is the resonance frequency. The experimental results for the magnetic contribution to the linewidth are plotted as a function of the magnetic susceptibility in Fig. 5(b) for Cr_7Fe. The linear relation predicted by Eq. (3) is well verified. In the fit of Fig. 5(b) we have neglected the nuclear dipolar contribution in Eq. (1) since at 1.5 T the inhomogeneous contribution to the width is already dominant. The values obtained from the fit for the average dipolar coupling is $A_z' = 27$ Hz/(G emu mol) corresponding to an hyperfine constant $A_z = (N_A/\gamma) A_z' = 3.82 \times 10^{21}$ cm^{-3}. This hyperfine constant corresponds to the dipolar interaction of a nucleus of ^1H with the electronic moment of a Cr^{3+} ion located at a distance of $r = 5$ Å or more. This distance is on the order of magnitude of the longest distances between protons and Cr ions in the molecule as seen from the structural data

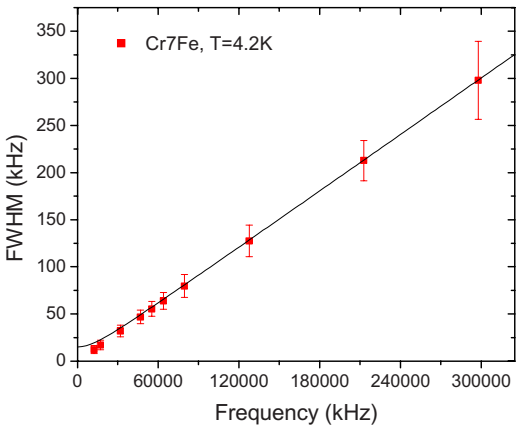

FIG. 6. (Color online) Proton NMR linewidth vs resonance frequency in Cr_7Fe at liquid Helium temperature. The full line is a fit according to Eqs. (1) and (3) as explained in the text.

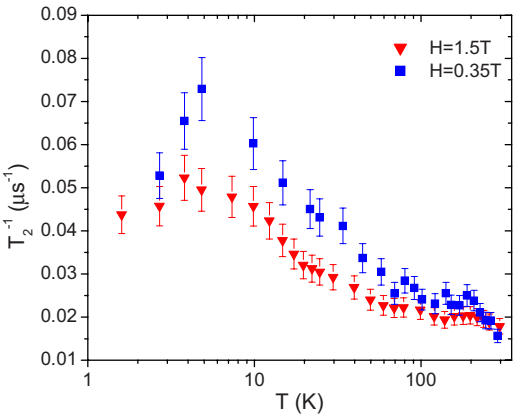

FIG. 7. (Color online) Proton spin-spin-relaxation rate T_2^{-1} as a function of temperature at two values of the external magnetic field for a polycrystalline sample of Cr_7Fe.

in Sec. II. This agrees with the notion that the NMR signal arises mainly from the protons furthest away and thus least magnetically coupled to the Cr(Fe) magnetic moments.

On lowering the temperature one expects a slowing down of the local moment fluctuations and for temperatures sufficiently low a freezing of the local moment on the time scale of the NMR hyperfine interactions which is on the order of 10^{-5} s. When this freezing occurs, one expects that the NMR width is no longer proportional to the external applied field.[9] In order to check the existence or not of freezing of the local moment at low temperature we have measured the field dependence of the linewidth at $T=4.2$ K. The results are shown in Fig. 6.

As can be seen from the Fig. 6 the linewidth is still proportional to the external field at Helium temperature, as predicted by Eq. (3), indicating that the fluctuations are still fast and the system behaves as a normal paramagnet. The data can be fitted using Eqs. (1) and (3) with $\langle \Delta\nu^2 \rangle_d = 15$ KHz and $A_z'\chi/\gamma = 0.001$ Hz/G. By using the value of the susceptibility at 4.2 K from Fig. 2, i.e., $\chi = 0.15$ emu/mol, one gets $A_z' = 28$ Hz/(G emu mol) corresponding to $A_z = (N_A/\gamma)A_z' = 3.9 \times 10^{21}$ cm^{-3} in good agreement with the value obtained from the fit of the data in Fig. 5, as expected since the hyperfine interaction should be almost temperature independent.

B. Temperature dependence of T_2^{-1} and wipe-out effect

The temperature dependence of the proton transverse relaxation rate as a function of temperature is shown in Fig. 7. As seen in the figure, T_2^{-1} increases on lowering the temperature. The shortening of T_2 is accompanied by a loss of signal intensity due to the limit of detectability of the NMR signal for short T_2 values (wipe-out effect) as is discussed below. The apparent maximum observed around 7–8 K is due to the fact that below 10 K the signal loss is severe and the measured T_2 is not representative of all nuclei but only of a small fraction having longer T_2 values.

The signal loss observed on lowering the temperature is described in Fig. 8. The wipe-out effect is a rather general phenomenon in NMR and has been observed previously in other systems such as spin glasses,[17] stripe-ordered cuprates,[18] and colossal magnetic resistance manganites.[19] In particular a loss of ^{1}H NMR signal on lowering the temperature has been observed previously in other molecular nanomagnets with a magnetic ground state and in that case also the wipe-out effect is correlated to an enhancement of the spin-spin-relaxation rate as in the present case.[9,20]

A quantitative analysis of the wipe-out effect was done successfully in Mn_6, Fe_4, and Fe_{19} molecular clusters[20] by using a simple and intuitive model which captures the main physical characteristics of the problem. We are going to analyze the wipe-out effect in Cr_7Fe by using the same model, which we summarize briefly in the following.

We assume that the dominant contribution to T_2^{-1} is coming from the dephasing due to the hyperfine interactions with the exchange coupled magnetic ions. In the weak collision, fast-motion approximation, the relaxation rate can be expressed in terms of the spectral density of the fluctuating hyperfine field at zero frequency as[15,21]

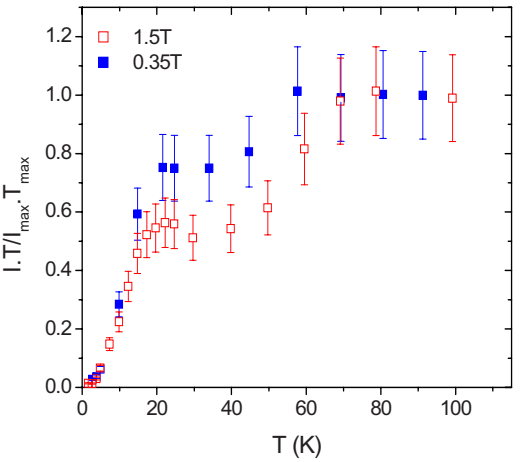

FIG. 8. (Color online) Proton NMR signal intensity multiplied by temperature plotted as a function of temperature for two external magnetic fields in polycrystalline Cr_7Fe. The decrease from the maximum value indicates that the observed signal at lower temperatures does not arise from all the nuclei present in the sample.

$$T_2^{-1} = \gamma_N^2 \langle \delta H_z^2 \rangle \tau(T) \propto \gamma_N^2 \frac{\langle \delta \mu_e^2 \rangle}{r^6} \tau(T), \quad (4)$$

where δH_z is the local longitudinal fluctuating field originating from a magnetic moment at a distance r from the proton spin, and τ gives the correlation time, which is solely determined by the dynamics of the exchange coupled magnetic ions and can thus be temperature dependent. The central idea is that, on lowering the temperature, the correlation time $\tau(T)$ becomes progressively longer and thus the relaxation rate T_2^{-1} becomes shorter [see Eq. (4)] until eventually it reaches the limiting value $\tau_d = 10^{-5}$ s, which we estimate to be the limit of detectability of the NMR signal in our experimental setup. Since the dipolar hyperfine field and thus T_2 depends on the distance r from the magnetic ions, the limiting value τ_d is reached progressively by all protons, with the ones closer being wiped out first.

To describe the wipeout we assume one central ion surrounded by a large number of protons homogeneously distributed at distances up to a maximum value R^*, the number density being $\rho = n_0/[(4\pi/3)(R^*)^3]$, where n_0 is the total number of protons in each molecule. Being in the regime of the wipe-out effect, and for a given temperature or value of the correlation time $\tau(T)$, there is a number of protons having a T_2^{-1} value larger than the critical value of 10^5 s^{-1}. These protons are enclosed within a notional sphere of radius $r_c(T)$ and do not contribute to the measured signal intensity. On the other hand, the protons located outside this sphere can be detected and their number $n(T)$ can be written as

$$n(T) = n_0 \left[1 - \left(\frac{r_c}{R^*} \right) \right]. \quad (5)$$

The value of the critical radius r_c in Eq. (5) can be obtained from Eq. (4) by setting $T_2^{-1} = \tau_d^{-1}$. Then one can express $n(T)$ in terms of the temperature-dependent correlation time $\tau(T)$ as

$$\frac{n(T)}{n_0} = 1 - \frac{\gamma_N \sqrt{\langle \delta \mu_e^2 \rangle \sqrt{\tau_d}}}{(R^*)^3} \sqrt{\tau(T)}. \quad (6)$$

In order to use Eq. (6) to fit the data in Fig. 8 one has to make some educated guess about the functional form of the temperature dependence of the correlation time $\tau(T)$. Previous NMR studies in a series of AFM rings have shown that the temperature dependence of the correlation time (extracted from the spin-lattice-relaxation data) has the form of a power law $\tau(T) = cT^{-3.5}$ for all the rings.[22] Therefore we adopt the same expression to fit the wipe-out data also for Cr_7Fe in Fig. 9, using Eq. (6). The two fitting parameters are the constant $c = 4 \times 10^{-6}$ s/rad and $\sqrt{\langle \delta \mu_e^2 \rangle}(R^*)^{-3} = 300$ G. The result of the fit is shown in Fig. 9 for the low-field data in which the wipe-out effect is more pronounced.

In view of the crudeness of the model the agreement appears satisfactory since the theoretical curve reproduces well the sudden drop in intensity occurring below 20 K. A qualitative confirmation of the model and of the fitting parameters used here will come from the analysis of the spin-lattice-relaxation rate T_1^{-1} presented in the next section. Finally it should be noted that the assumption of a single correlation time and of the consequent temperature-dependence law for $\tau(T)$ may be an approximation in heterometallic rings worse than in homometallic rings and clusters since in the first case one expects multiexponential behavior of the electron spin-correlation function due to the size distribution of local moments in the ring.

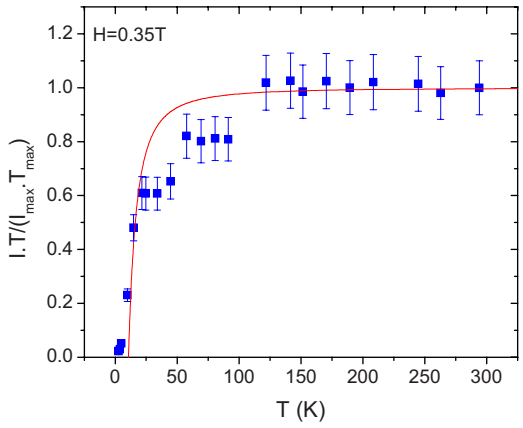

FIG. 9. (Color online) Fit of the wipe-out effect in Cr_7Fe using Eq. (6) with the following fitting parameters: $c = 4 \times 10^{-6}$ s/rad and $\sqrt{\langle \delta \mu_e^2 \rangle}(R^*)^{-3} = 300$ G.

C. Temperature dependence of T_1^{-1}

The temperature dependence of the proton average spin-lattice-relaxation rate is shown in Fig. 10 for two values of the external magnetic field. The main qualitative feature is the presence of a field-dependent peak at low temperature. This peak is typical of all molecular magnetic homometallic rings and clusters.[9,22] A quantitative theoretical explanation of the peak was given before in terms of the relaxation of the magnetization due to spin-phonon interactions.[23] A subsequent theoretical analysis has provided an explanation for the origin of the universal behavior of the slowing down of the magnetization fluctuations, which is responsible for the observed peak.[24] In this experimental paper we analyze the data

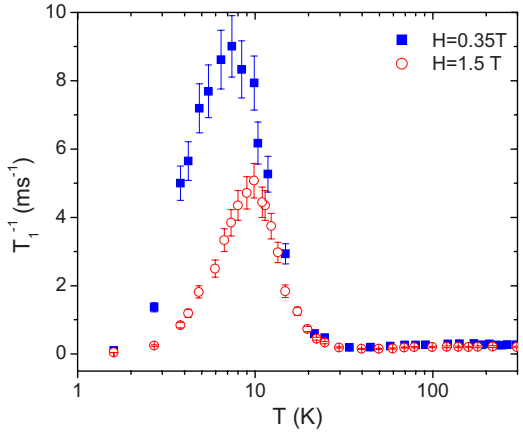

FIG. 10. (Color online) Proton average spin-lattice-relaxation rate plotted vs temperature for two external magnetic fields in a Cr_7Fe powder sample.

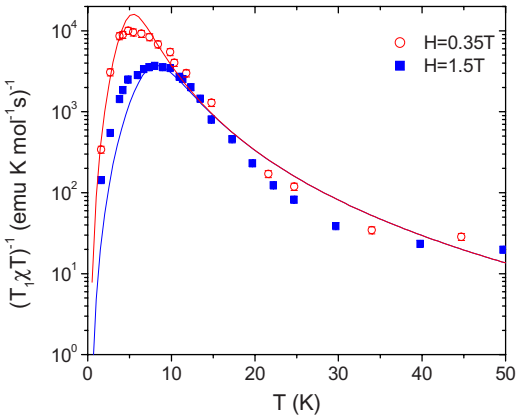

FIG. 11. (Color online) Proton spin-lattice-relaxation rate divided by χT vs temperature for Cr_7Fe at two values of the external field. The curves are fitted using Eq. (7) with $A=3.0\times10^9$ (ms^{-1} rad)^2, a fitting parameter obtained from the high field data, and $\omega_c=2.5\times10^5T^{3.5}$ as obtained from the fit of the wipe-out effect in FIG. 9.

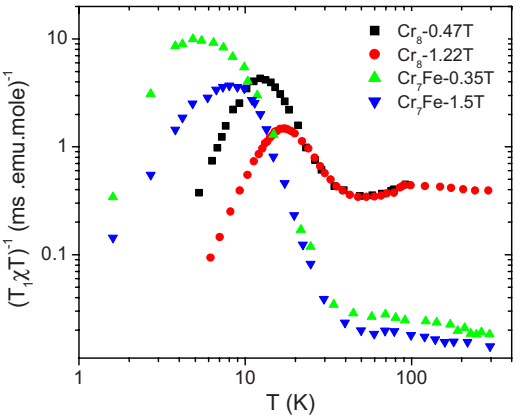

FIG. 12. (Color online) Comparison of the proton relaxation data in Cr_7Fe with the published data in homometallic ring Cr_8 (Ref. 22).

in a phenomenological way using a single-correlation frequency to describe the electronic spin dynamics in the same way as done in Ref. 22. This will allow us to capture the relevant changes occurring in the spin dynamics when comparing the results in the heterometallic ring Cr_7Fe with the homometallic one Cr_8.

In order to fit the data in Fig. 10 we refer to the simple expression for the relaxation rate, which can be obtained from the original Moriya theory of nuclear relaxation in paramagnets[15,21] under some simplifying assumptions, the main one being that the electronic spin dynamics is dominated by a single-correlation frequency, which drives the longitudinal electron spin fluctuations.[22,23] The expression is

$$\frac{1}{T_1}=A'\frac{\omega_c(T)}{\omega_c^2(T)+\omega_L^2}=A\chi T\frac{\omega_c(T)}{\omega_c^2(T)+\omega_L^2}, \tag{7}$$

where $A\chi T$ is the average square of the fluctuating transverse hyperfine field, ω_L is the proton Larmor frequency, $\omega_c(T)=1/\tau(T)$ is the characteristic frequency, and χ is the uniform magnetic susceptibility expressed in emu/mole. The temperature dependence of χT (see Fig. 3) represents the amplitude of the local effective moments. Thus in order to extract the dynamics, it is best to plot $(T_1\chi T)^{-1}$ versus temperature, as shown in Fig. 11. The data can now be fitted with two fitting parameters: A which represents the average square of the nuclear electron hyperfine fluctuations and $\omega_c(T)$ which can be assumed to be of the form $\omega_c(T)=\tau(T)^{-1}=c^{-1}T^{3.5}$ to be consistent with the wipe-out analysis of the previous paragraph and the results in other AFM rings.[22]

As one can see in Fig. 11, the theoretical curve given by Eq. (7) reproduces qualitatively the relaxation data by using only one single fitting parameter, namely, $A=3.0\times10^9$ (ms^{-1} rad)^2 while for the correlation frequency we used the value obtained from the analysis of the wipe-out effect. One should note that a good fit for temperatures less than 10 K is impossible anyway since the data at low temperature are affected by the wipe-out effect and thus they do not represent an average relaxation rate over all protons of the molecule. The value of the squared hyperfine interaction A can be compared with the hyperfine interaction obtained from the fit of the linewidth data in Figs. 5 and 6. To do so one has to convert the units by recalling that $A_{\pm}^2=A/4\pi(\hbar\gamma_n\gamma_e)^2=1.44\times10^{44}$ cm^{-6} corresponding to $A_{\pm}=1.2\times10^{22}$ cm^{-3}. This value for the transverse hyperfine field, $A_{\pm}$, compares well with the value obtained from the linewidth for the longitudinal hyperfine field A_z. This is a confirmation that both the temperature-dependent inhomogeneous broadening and the spin-lattice-relaxation are driven by the nuclear electron dipolar interaction.

As anticipated in the previous section, it must be remarked that two assumptions made here, based on previous work in homometallic AFM rings, could be subject to criticism. One regards the assumption of a single-correlation function since it was found that in heterometallic rings, particularly in the temperature region of the peak in T_1^{-1}, the spin-spin-correlation function shows a multi-Lorentzian regime.[25,26] The second assumption is the one leading to the proportionality of T_1^{-1} to χT [see Eq. (7)]. Both effects are the consequence of a nonuniform distribution of the local magnetic moments in the heterometallic rings.

V. DISCUSSION AND CONCLUSIONS

One of the aims of the present work is to study the effect of the heterometallic substitution on the spin dynamics in the AFM ring. The strong effect on the spin dynamics as the result of the heterometallic substitution of one Cr atom with a Fe atom in the ring can be seen directly by comparing the proton relaxation rates in Cr_7Fe and in Cr_8 at similar values of the external magnetic fields, as shown in Fig. 12. As can be seen from the figure, at comparable values of the external magnetic field, the relaxation in heterometallic rings displays a maximum shifted by several degrees towards lower temperature compared with the data in the homometallic ring. Furthermore the results at high temperature ($T>40$ K) differ by more than one order of magnitude.

Another more quantitative way to compare the spin dynamics in heterometallic and homometallic ring can be done

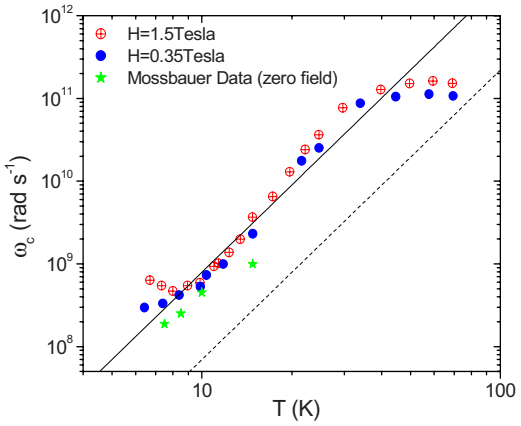

FIG. 13. (Color online) Correlation frequencies for Cr_7Fe extracted from the NMR experimental data compared with the ones obtained from Mossbauer data, Ref. 27, plotted vs temperature. The full line corresponds to the behavior $\omega_c(T)=2.5\times10^5T^{3.5}$ rad/s obtained from the relaxation and wipe-out effect (see FIG. 11). The dashed line corresponds to the behavior found in Cr_8, i.e., $\omega_c(T)=2.2\times10^4T^{3.5}$ rad/s (Ref. 20).

by extracting the temperature dependence of the correlation frequency $\omega_c(T)$ from the experimental NMR relaxation data $(T_1\chi T)^{-1}$ in Fig. 11 and using Eq. (7). As shown in Fig. 13 this correlation frequency follows rather well the power-law temperature dependence in the intermediate temperature range. At low temperature the results are not reliable because of the wipe-out effect while at high temperature the deviation is probably due to additional relaxation mechanisms not included in Eq. (7). The two important points are first, that our results obtained from proton NMR are in good agreement with the results obtained from the temperature dependence of the width of the Mossbauer spectrum[27] and second, that the correlation frequency in Cr_7Fe seems to be one order of magnitude higher than in Cr_8 (dashed line in Fig. 13). This last point is important because it indicates that the heterometallic substitution has a strong effect on the spin dynamics.

By concluding we can say that the magnetic-susceptibility measurements show that the heterometallic ring Cr_7Fe displays a magnetic ground state with $S_T=1/2$. The Cr-Cr exchange interaction as derived from the high-temperature magnetization data is found to be comparable to the one found in other heterometallic rings and in Cr_8, while the exchange interaction Cr-Fe cannot be determined from our data alone. The proton NMR inhomogeneous linewidth and the spin-lattice-relaxation rates are driven by the dipolar interaction of nuclei with the magnetic moment of the paramagnetic ion. The NMR results, including the wipe-out effect, can all be explained qualitatively with the known theoretical formula and in terms of a single temperature-dependent correlation frequency, which characterizes the spin dynamics in the AFM rings. The spin dynamics appears to be faster by one order of magnitude in Cr_7Fe with respect to Cr_8. This is a central result of the present work. According to previous theoretical work,[23,24] the correlation frequency for the electron spin fluctuations should be driven by spin-phonon interaction. It is remarked again that the simple description in terms of a single-correlation frequency [see Eq. (7)] may be inadequate in presence of a distribution of different sizes of local moments as expected in heterometallic rings. A refined theoretical analysis, now in progress, will take into account the exact expression of the hyperfine fluctuations, the different dominating correlation times and the changes in elastic properties with respect to homometallic rings.[26]

ACKNOWLEDGMENTS

The authors are grateful to P. Santini, S. Carretta, and G. Amoretti for useful discussions and suggestions. Thanks are also due to L. Cianchi, M. Lantieri, and G. Spina for discussions and making available the Mossbauer data before publication. The present work was done with financial support from the NoE-MAGMANET network of the European community and PRIN-200609518 project of the Italian Ministry of Research.

*Corresponding author; houshang.amiri@unipv.it

[1] O. Kahn, *Molecular Magnetism* (VCH, Berlin, 1990); D. Gatteschi, R. Sessoli, and J. Villain, *Molecular Nanomagnets* (Oxford University Press, New York, 2006).

[2] I. S. Tupitsyn and B. Barbara, in *Magnetism: Molecules to Materials III*, edited by J. Miller and M. Drillon (Wiley, New York, 2002).

[3] E. del Barco, A. D. Kent, S. Hill, J. M. North, N. S. Dalal, E. M. Rumberger, D. N. Hendrickson, N. Chakov, and G. Christou, J. Low Temp. Phys. **140**, 119 (2005); W. Wernsdorfer, Adv. Chem. Phys. **99**, 118 (2001).

[4] M. Affronte, T. Guidi, R. Caciuffo, S. Carretta, G. Amoretti, J. Hinderer, I. Sheikin, A. G. M. Jansen, A. A. Smith, R. E. P. Winpenny, J. van Slageren, and D. Gatteschi, Phys. Rev. B **68**, 104403 (2003).

[5] F. K. Larsen, E. J. L. McInnes, H. ElMkami, J. Overgaard, S. Piligkos, G. Rajaraman, E. Rentschler, A. A. Smith, G. M. Smith, V. Boote, M. Jennings, G. A. Timco, and R. E. P. Winpenny, Angew. Chem., Int. Ed. **42**, 101 (2003).

[6] E. Micotti, Y. Furukawa, K. Kumagai, S. Carretta, A. Lascialfari, F. Borsa, G. A. Timco, and R. E. P. Winnpenny, Phys. Rev. Lett. **97**, 267204 (2006).

[7] F. Troiani, M. Affronte, S. Carretta, P. Santini, and G. Amoretti, Phys. Rev. Lett. **94**, 190501 (2005); F. Troiani, A. Ghirri, M. Affronte, S. Carretta, P. Santini, G. Amoretti, S. Piligkos, G. Timco, and R. E. P. Winpenny, *ibid.* **94**, 207208 (2005).

[8] G. A. Timco, S. Carretta, F. Troiani, F. Tuna, R. J. Pritchard, E. J. L. McInnes, A. Ghirri, A. Candini, P. Santini, G. Amoretti, M. Affronte, and R. E. P. Winpenny, Nat. Nanotechnol. **4**, 173 (2009).

[9] F. Borsa, A. Lascialfari, and Y. Furukawa, in *Novel NMR and EPR Techniques*, edited by J. Dolinsek, M. Vilfan, and S. Zumer

(Springer, New York, 2006).
[10] N. V. Gerbeleu, Yu. T. Struchkov, G. A. Timco, A. S. Batsanov, K. M. Indrichan, and G. A. Popovich, Dokl. Akad. Nauk SSSR **313**, 1459 (1990).
[11] J. van Slageren, R. Sessoli, D. Gatteschi, A. A. Smith, M. Helliwell, R. E. P. Winpenny, A. Cornia, A.-L. Barra, A. G. M. Jansen, G. A. Timco, and E. Rentschler, Chem.-Eur. J. **8**, 277 (2002).
[12] M. Affronte, A. Ghirri, S. Carretta, G. Amoretti, S. Piligkos, G. A. Timco, and R. E. P. Winpenny, Appl. Phys. Lett. **84**, 3468 (2004).
[13] A. Bianchi, S. Carretta, P. Santini, G. Amoretti, Y. Furukawa, K. Kiuchi, Y. Ajiro, Y. Narumi, K. Kindo, J. Lago, E. Micotti, P. Arosio, A. Lascialfari, F. Borsa, G. Timco, and R. E. P. Winpenny, J. Magn. Magn. Mater. (to be published).
[14] R. Caciuffo, T. Guidi, G. Amoretti, S. Carretta, E. Liviotti, G. Amoretti, S. Piligkos, G. Timco, C. A. Muryn, and R. E. P. Winpenny, Phys. Rev. B **71**, 174407 (2005).
[15] C. P. Slichter, *Principles of Magnetic Resonance* (Springer-Verlag, Berlin, 1996).
[16] P. Khuntia, M. Mariani, M. C. Mozzati, L. Sorace, F. Orsini, A. Lascialfari, F. Borsa, C. Maxim, and M. Andruh, Phys. Rev. B **80**, 094413 (2009).
[17] D. A. Levitt and R. E. Walstedt, Phys. Rev. Lett. **38**, 178 (1977).
[18] A. W. Hunt, P. M. Singer, K. R. Thurber, and T. Imai, Phys. Rev. Lett. **82**, 4300 (1999).
[19] G. Papavassiliou, M. Belesi, M. Fardis, and C. Dimitropoulos, Phys. Rev. Lett. **87**, 177204 (2001).
[20] M. Belesi, A. Lascialfari, D. Procissi, Z. H. Jang, and F. Borsa, Phys. Rev. B **72**, 014440 (2005).
[21] T. Moriya, Prog. Theor. Phys. **16**, 23 (1956).
[22] S. H. Baek, M. Luban, A. Lascialfari, E. Micotti, Y. Furukawa, F. Borsa, J. van Slageren, and A. Cornia, Phys. Rev. B **70**, 134434 (2004).
[23] P. Santini, S. Carretta, E. Liviotti, G. Amoretti, P. Carretta, M. Filibian, A. Lascialfari, and E. Micotti, Phys. Rev. Lett. **94**, 077203 (2005).
[24] I. Rousochatzakis, A. Lauchli, F. Borsa, and M. Luban, Phys. Rev. B **79**, 064421 (2009).
[25] A. Bianchi, S. Carretta, P. Santini, G. Amoretti, J. Lago, M. Corti, A. Lascialfari, P. Arosio, G. Timco, and R. E. P. Winpenny (unpublished); A. Bianchi *et al.*, J. Magn. Magn. Mater. (to be published).
[26] P. Santini *et al.* (unpublished).
[27] M. Lantieri, L. Cianchi, F. Del Giallo, P. Moretti, G. Spina, and G. Timco, J. Phys.: Conf. Ser. (to be published); (private communication).